On The Construction Of Linear Induction MHD Generators With Optimized Coil System And Optimal Conductivity Of The Working Fluid

Author(s): C. Carpetis

Session Name: Liquid Metal MHD Generators

SEAM: 8 (1967)

SEAM EDX URL: https://edx.netl.doe.gov/dataset/seam-8

EDX Paper ID: 215

ON THE CONSTRUCTION OF LINEAR INDUCTION MHD GENERATORS WITH OPTIMIZED COIL SYSTEM AND OPTIMAL CONDUCTIVITY OF THE WORKING FLUID

C. Carpetis
Deutsche Versuchsanstalt für Luft- und Raumfahrt e.V.
Stuttgart-Vaihingen, Germany

Abstract

Introduction

In most cases where use of induction MHD generators with fluid metal (Figures 1, 9) as the working fluid is considered, a high power density is required. Hence there is a great need for optimizing this machine, and therefore the typical differences between the MHD machine and the conventional asynchrone machine must be taken into consideration. The most important differences are:

- 1. The gap between iron cores in the MHD machine is very large, and this diminishes the power factor.
- 2. Because of the open conditions of the winding system, end effects occur which diminish the net power.

In the following paragraphs proposals are made to minimize the influence of the above characteristics, and some experimental investigations are reported.

The Influence of the large Gap and the Use of Cryogenically Cooled Windings

Numerical evaluation of the machine performance, based on the determination of the impedance of the machine (1,2), has shown that the power factor $\cos \phi$ is very low because of the low main reactance) and that unacceptably high ohmic losses occur in the coils if the power density is to be acceptable.

A possibility to overcome the resulting difficulties is given by the use of cryogenics for cooling of the coil system(2,3). We can show the advantages of this method on the graph of the factor w (Figure 2). It is

 $w = \frac{\rho(T)}{\rho(T_0)} \left[1 + \frac{1}{\eta(T)} \frac{T_0 - T}{T}\right]$

and hence w is equal to the ratio of the ohmic losses in the coils plus the power of the needed heat pump by use of cryogenic cooling to the losses of the same machine with conventional winding system (4).

The factor w can be diminished down to 15% if the temperature of the coils is held to cryogenic region. It is evident that the most suitable material for the coils would be beryllium(5) at 70°K.

Nevertheless, in Figures 3, 4, and 5, an MHD generator model using aluminum for the cryogenic cooled coil system is compared to a model of the same dimensions using a conventional winding system. The comparison shows that a cryogenically cooled machine produces a much higher power with

better power factor, and it has a higher power density, even if the mass and the power of the heat pump are added.

The Influence of the End Effects and the Selection of Optimal Conductivity

In the above investigation end effects are not taken into consideration, but this is allowed because only the temperature of the windings is to be optimized. But for the determination of the real performance of the machine, the consideration of the end effects is of major importance. A complete theoretical investigation of the problem based on the two-sided Laplace-Transform is given in Reference 6. The numerical evaluation of this theory for an MHD model of constant length L with NaK as the working fluid leads to the current diagrams of Figures 6 and 7a.

Comparison of the performance for p=2, p=4, p=6 shows that:

- 1. The real performance of the machine is much different from the ideal performance (without consideration of end effects) for small pole-numbers p, but neglectable for p greater than 6.
- for p greater than 6.

 2. The real performance has an optimum with p=4 (Figure 7b). (Ideal performance would be optimal for p=1!) But the influence of the end effects is shown to be a function of the conductivity. So, if we consider Hg as the working fluid in the same machine, the optimum performance is found for p=2 (Figure 8).

In Figure 8 the optimum performance possible with NaK (for p = 4) is compared to the optimum performance possible with Hg (for p = 2) as the working fluid in the same machine. The comparison shows that the performance in the second case (with Hg) is better. It is evident that the better performance in the second case is due to the better ratio $\sqrt[3]{a}$ because p could be selected p = 2. But if the conductivity is higher, the end effects are very strong for lower values of p, and one finds that it must be p=4 for the optimum performance. But for p = 4 the ratio $\sqrt[n]{a}$ is four times smaller than in the first case. It follows that in order to design an MHD machine with an optimal performance, a simultaneous optimization of two parameters (pole-pair number p and conductivity of the working fluid o) based on the above theory (References 6 and 7) is needed.

Experimental Facility and Results of Empty Channel Measurements

An experimental MHD converter with Hg as the working fluid built in the DVL-Institute for Energy Conversion is shown in Figure 9. The three-phase winding system is made from copper tubes so that cryogenic cooling with liquid nitrogen is possible, and it is provided that the wavelength of the magnetic field, being normally $\lambda=0.20$ m, can be easily changed over to $\lambda=0.40$ m. Some information about this machine is given in Table 1. Until the present time, the empty channel measurements include the determination of the impedance for various wavelengths and numbers of wavelengths and investigations of the magnetic field in the middle plane of the channel.

Table 1 V = 380 V f = 50 Hz b = 0.080 m = 0.40 m or 0.20 m a = 0.005 m = 0.019 L = 1.6 m N = 1080/m

Some results of these measurements are the following:

1. If the wavelength remains constant, the magnetic relations in the short-stator machine do not depend on the length of the machine (i.e., on the number of the polenging n)

pairs p). 2. If the length of the short-stator re remains constant, the reactance of the machine can be increased by increasing the ratio \sqrt{a} , i.e., by increasing the wavelength (Figures 10a and 10b for L = 1.6 m). But there is an upper limit of this ratio when the working fluid is interacting in the channel, which must be determined by means of the theory of the end effects (see preceding section).

3. The field distribution for empty channel condition is shown in Figure 11 for p = 8, 5, 3 and λ = 0.20 m. The travelling wave (λ = 20 cm) as photographed for three instants of the polyphase cycle and for p = 8, 5, 4 is shown in Figure 12*. It is shown that, as the wave is travelling, the end disturbances change their form but they do not practically exceed more than a wavelength. Furthermore, they are the same for all lengths of short-stators and for even or odd numbers of pole-pairs.

Conclusions

Two typical characteristics of the linear inductive MHD machine, the large gap and the short-stator, highly influence the performance of the linear induction MHD generator machine. Cryogenic cooling of the coils is proposed as a means of increasing the power density of the machine. The end effects, resulting from the short-stator conditions of the machine, can be minimized by the optimal choice of two parameters: wavelength and conductivity of the working fluid.

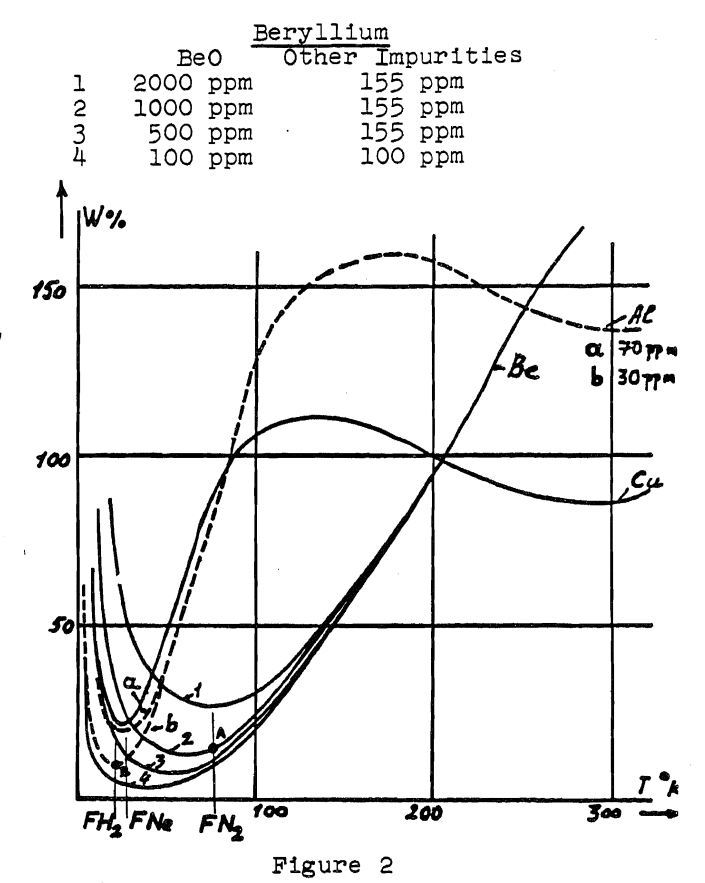
References

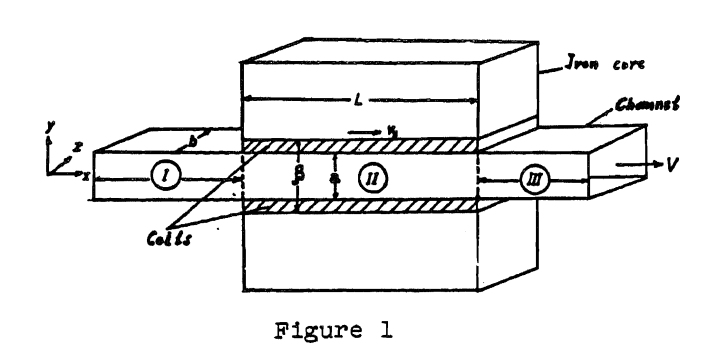
- Jackson, W. D. and Pierson, E. S.,
 "Operating Characteristics of the
 MHD Induction Generator," Symposium
 on Magnetoplasmadynamics Electrical
 Power Generation, University of Durham,
 Newcastle-upon-Tyne, Sept. 1962.
- Peschka, W., Carpetis, C., and Engeln, F., "Das Betriebsverhalten eines ebenen elektrodenlosen MHD-Wandlers mit kryogen gekühlter Primärwicklung,"
 Flugwissenschaften 14, 81-89 (Feb. 1966).
- Peschka, W., Carpetis, C., Gann, A., and Tries, B., "On Some Aspects on the Use of a Cryogenically Cooled Primary Windings System for an AC-MHD-Generator," International Symposium on MHD Electrical Power Generation, Salzburg, July 1966.
- 4. Burnier, P. and de la Hurpe, A.,
 "Applications de l'Hydrogene Liquide
 en Electrotechnique," Cours sur l'
 Hydrogene Liquide, Grenoble, June 1965.
- 5. Vachet, P., "Le Béryllium et les Cryomachines," Revue Générale de l' Electricité, June 1965.
- 6. Engeln, F. and Peschka, W., "End Effects on the Linear Induction MHD-Generator Calculated by Two-Sided Laplace Transform," International Symposium on MHD Electrical Power Generation, Salzburg, July 1966.
- 7. Engeln, F. and Peschka, W., "Die Lösung einer speziellen elliptischen linearen partiellen Differentialgleichung zweiter Ordnung mit Hilfe der zweiseitigen Laplace-Transformation," ZAMM, GAMM-Tagungs-Sonderheft, 1966.

In the photographs of Figure 12 the oscillograms are shown symmetrical to the horizontal axis because the Y-display indicated the a.c. voltage induced in the probe coil, and rectifying was not convenient or desirable.

Nomenclature

channel height a ъ channel width fIJL frequency current phasor $j = \sqrt{-1}$ total length of the machine Ν conductors number per unit of length (in the coils) Ρ number of pole-pairs or wavelengths p corresponding to the machine-length L s T To slip temperature (°K) 370°K U U voltage voltage phasor phase voltage Uph $\overline{\sigma}_R$ ohmic component of U $\mathbf{u}_{\mathbf{B}}$ inductive component of U z impedance reactance $\eta(T)$ ratio of the efficiency of the heat pump to the efficiency of the Carnot-cycle working between T and To wavelength ρ(T) resistivity at temperature T conductivity angle between $\overline{\mathbf{I}}$ and $\overline{\mathbf{U}}$ φ





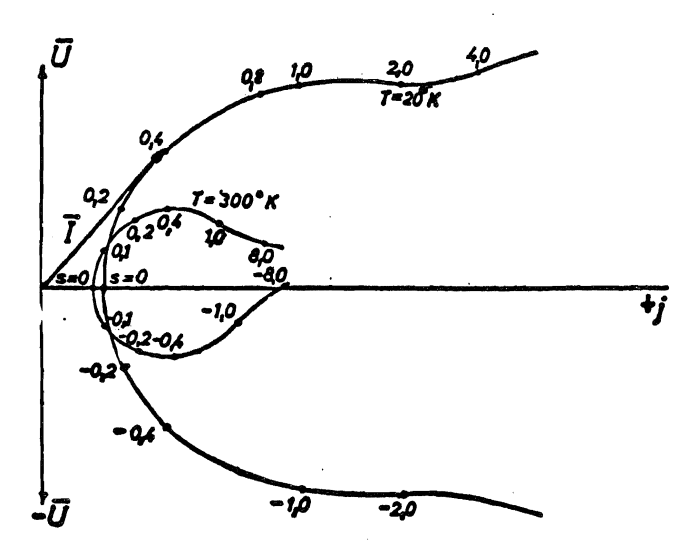


Fig. 3 Current Phaser Location Diagrams of an MHD Machine
(a) with cryogenically cooled windings system at 20°K
(b) with conventional winding system.

The parameter is the slip s.

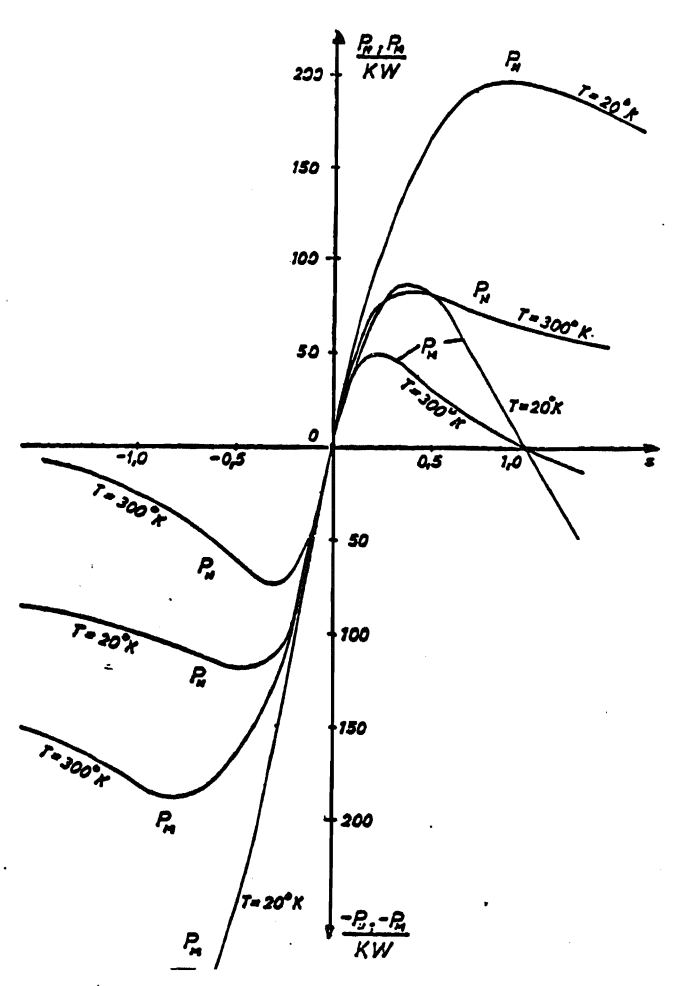


Fig. 4 Mechanical Power P_M and Network

Power P_N as a Function of the
Slip s for an MHD Machine
(a) with cryogenically cooled
windings at 20°K
(b) with conventional winding

(b) with conventional windi system.

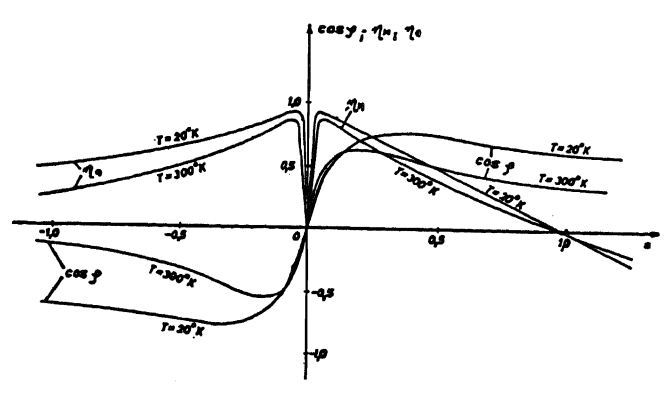


Fig. 5 Power Factor and Efficiency as a Function of the Slip s for an MHD Machine

- (a) with cryogenically cooled Winding system
- (b) with conventional winding system

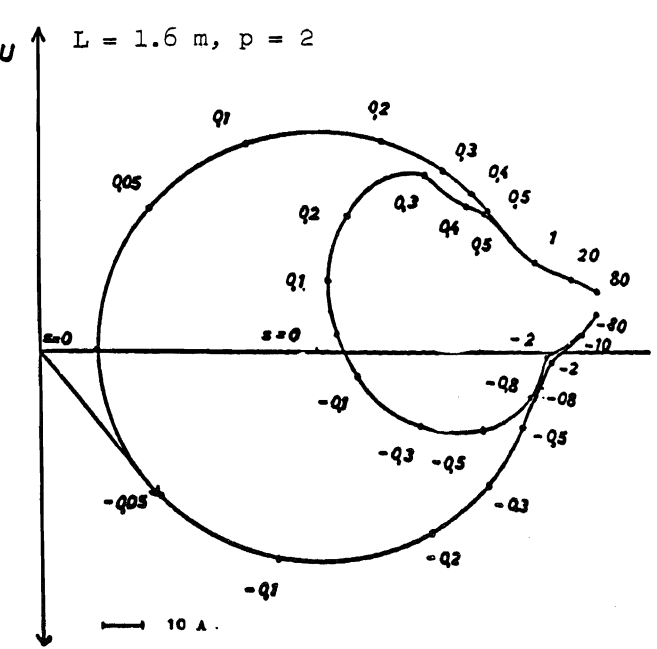
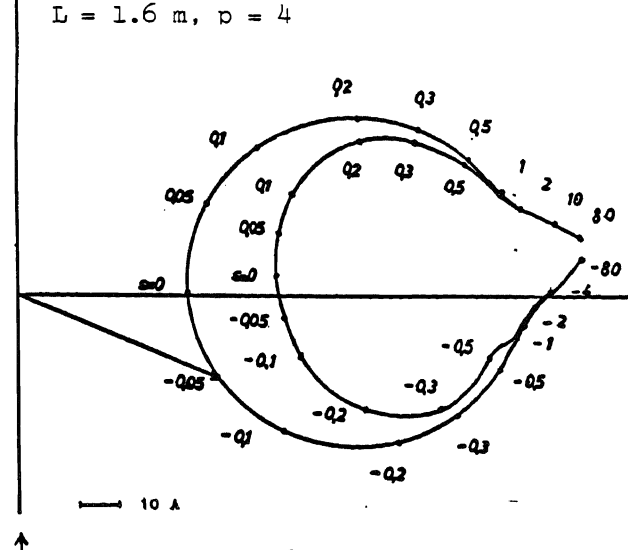


Fig. 6 Current Phaser Location Diagram (parameter: slip s) for an MHD Machine (a) with the end effects taken into account

(inner diagram)

(b) without consideration of the end effects (outer diagram)



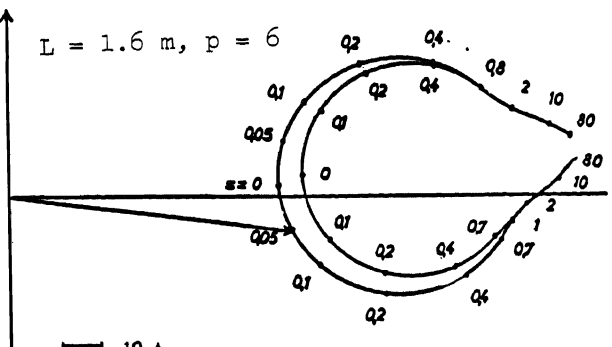


Fig. 7a Current Phaser Location Diagram (parameter: slip s) for an MHD Machine

- (a) with the end effects taken into account (inner diagram)
- (b) without consideration of the end effects (outer diagram)

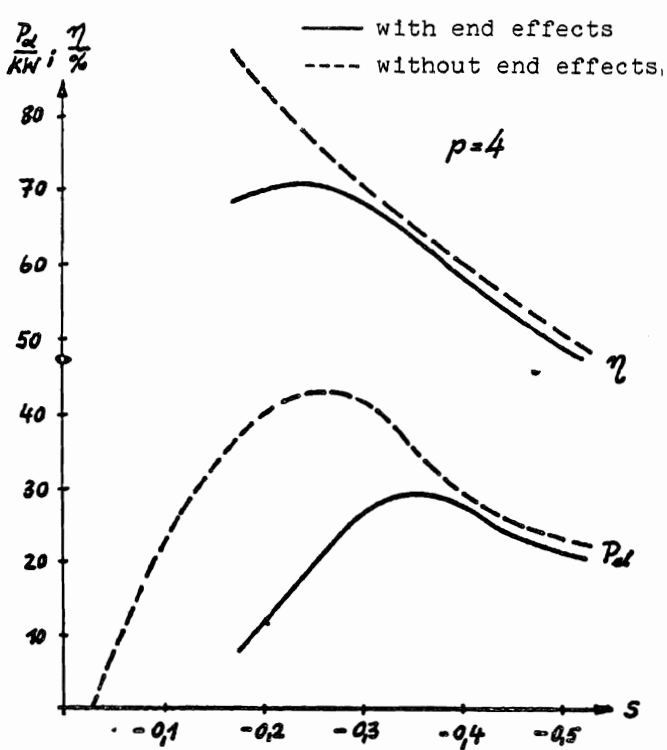
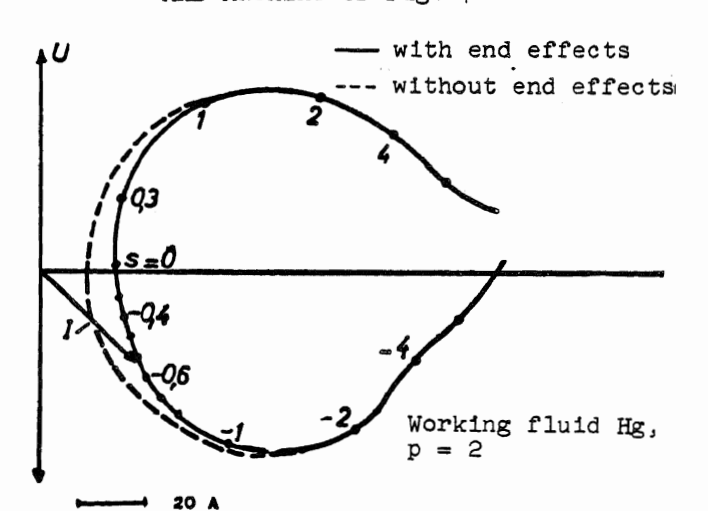


Fig. 7b Net Power and Efficiency of the MHD Machine of Fig. 7a



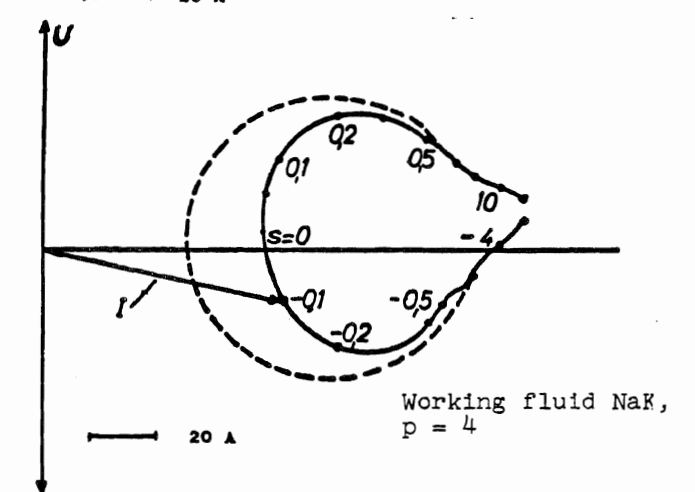


Fig. 8 Optimal Current Phaser Diagrams for Hg or NaK

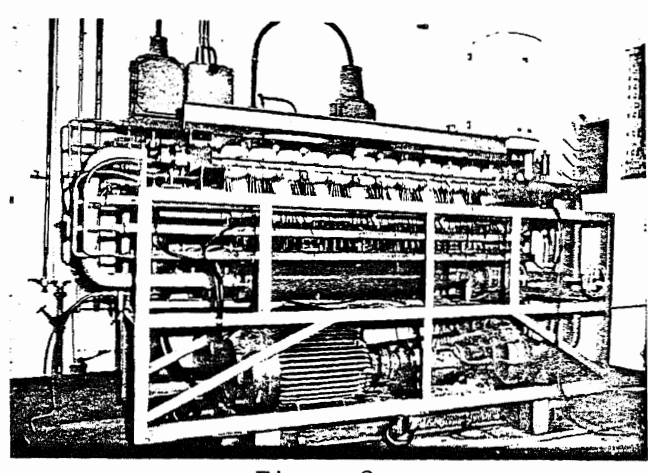


Figure 9

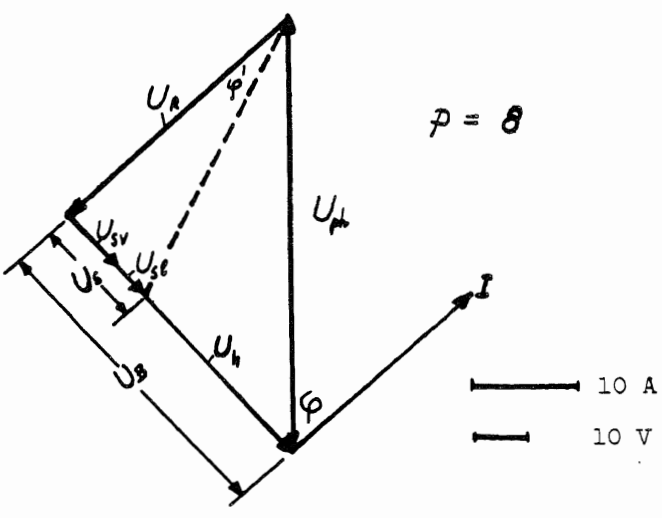


Figure 10a

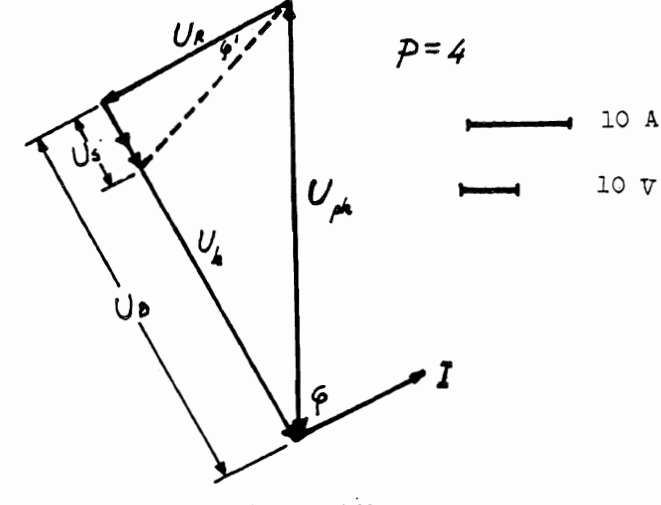


Figure 10b

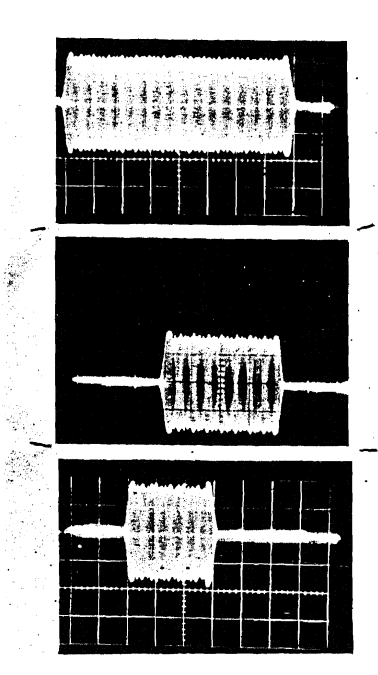


Figure 11

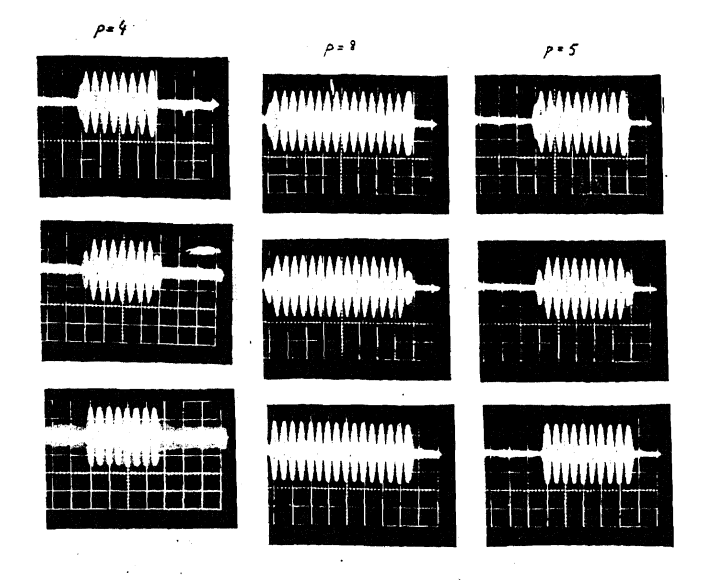


Figure 12